Momentum Budgets of a Subtropical Squall Line Determined from Dual-Doppler Data

YEONG-JER LIN, HSI SHEN, FANG-CHEN CHENG
Department of Earth and Atmospheric Sciences
Saint Louis University, St. Louis, MO 63103 U.S.A.
AND
ROBERT W. PASKEN
Department of Mathematics, Parks College of
Saint Louis University, Cahokia, IL 62206 U.S.A.

(Received 4 October 1990; revised 24 December 1990)

ABSTRACT

A thermodynamic retrieval method was employed to investigate some structural features of a subtropical squall line during IOP-2. Dual-Doppler data, centered at 0040, 0043, 0046, 0049, and 0052 LST 17 May 1987, were objectively analyzed in the horizontal domain of 45 km by 25 km using 1 km grid spacing. There were 10 analysis levels in the vertical ranging from 0.3 to 8.8 km. Vertical velocities were computed from the anelastic continuity equation by integrating downward with variational adjustment. Fields of deviation perturbation pressure and temperature were retrieved from the Doppler derived winds using the three momentum equations. These fields were subjected to internal consistency checks to determine the level of confidence before interpretation.

Results show that the vertical transport of horizontal momentum normal to the line is downward corresponding to the west-tilted convective updrafts, while the line-parallel component results in an upward momentum transport. Momentum budget calculations show that the horizontal and vertical flux convergences/divergences of horizontal momentum by the mean and eddy motions contribute largely to the growth/decay of mean horizontal momentum. These findings are in qualitative agreement with those of tropical squall lines during COPT 81. The dynamic interaction between the mesoscale convective system and its environment can be studied using the momentum budget equations and vertical fluxes of horizontal momentum estimated from the Doppler derived winds.

1. INTRODUCTION

The momentum transport by a line of comulonimbus observed by aircraft during GATE (GARP Atlantic Tropical Experiment) off the west coast of Africa was investigated by LeMone (1983). She found that the vertical transport of horizontal momentum normal to this line of cumulonimbus was against the vetical momentum gradient, contrary to mixing-length theory predictions. Conversely, the vertical transport of horizontal momentum parallel to the axis of the convective band was along the vertcial momentum gradient as predicted by the theory. In the later study, LeMone *et al.* (1984) found that the mesoscale tropical convective line increases front-to-rear momentum at heights $> 4\ km$, and rear-to-front momentum at lower levels. The vertical transport of horizontal momentum parallel to the convective line axis was downgradient, and the vertical flux of horizontal momentum normal to the line was independent of the vertical shear of the horizontal wind.

Momentum fluxes across the line of the mesoscale convective system (MCS), which occurred off the southeast coast of Taiwan on 16 June 1987, were investigated by LeMone and Jorgensen (1989) using the TAMEX (Taiwan Area Mesoscale Experiment) P-3 arircraft and airborne Doppler data. They found that the u-momentum flux was negative below $4\ km$, and positive above. Because the line and its constituent updrafts were not moving in an east-west direction, this was consistent with the westward tilt of the observed updrafts below $4\ km$ and their eastward tilt higher up.

Using the dual-Doppler data collected during TAMEX-IOP 2, Lin et al. (1990) investigated the vertical transports of horizontal momentum for a subtropical squall line embedded within the MCS over the Taiwan Straits. Results showed that the vertical component of horizontal momentum flux normal to the line is downward from the surface to $6.5\ km$ with a maximum near $3\ km$. This finding is in qualitative agreement with those reported in GATE and other studies, and is consistent with the westward-tilted updrafts in the layers between the surface and $5\ km$. On the other hand, the vertical transport of horizontal momentum parallel to the line is upward at heights $< 6.5\ km$ with a maximum at the LLJ (low-level jet) level and is downward higher up.

The momentum budget for the u-component normal to a tropical squall line was investigated by Lafore *et al.* (1988) using a three-dimentional cloud model. A comparison was made between the computed budget and the observed one determined from the Doppler data during COPT 81 (Convection Profonde Tropicale). Results showed that the contributions from the three advection terms are dominant over the other terms in the budget equation. The horizontal advection terms have the same order of magnitude as the vertical term, but the sign is opposite. These findings are in good qualitative agreement with those

reported in the study by Lin *et al.* (1990) using the TAMEX dual-Doppler data.

The current study is an extension of the study by Lin *et al.* (1990) for the same 17 May case in IOP-2. The vertical transports of horizontal momentum for components normal to and parallel to the leading edge of a subtropical squall line are computed from the Doppler derived winds at five consecutive analysis times in intervals of about 3 min. Subsequently, the momentum budgets for both u- and v-components, averaged over the horizontal domain of interst, are obtained using the derived wind and pressure fields. The goal is to better understand the structure and internal dynamics of a subtropical squall line that produced heavy precipitation on the northwest coast of Taiwan during the Mei-Yu season.

2. THE SQUALL SYSTEM

As described in studies by Wang *et al.* (1990) and Lin *et al.* (1990), dual-Doppler data from the CP-4 and TOGA radars at 0040, 0043 and 0046 LST (local standard time) 17 May 1987 were used to study the structure and internal dynamics of a subtropical squall line. These data were objectively analyzed in the horizontal domain of 25 km by 41 km covering the convective region of the line. There were 10 analysis levels in the vertical ranging from 0.3 to 8.8 km. The horizontal and vertical grid spacing was 1 km except for the lowest two levels, where δz was chosen to be 0.5 km. Vertical velocities were calculated from the anelastic continuity equation by integrating downward with variational adjustment.

Once the three-dimensional wind field was derived, fields of deviation perturbation pressure and virtual temperature were retrieved from the Doppler derived winds using the three momentum equations (e.g., Lin *et al.*, 1986). The retrieved field was subjected to momentum checking to determine the level of confidence before interpretation.

Results showed that many structural features of a subtropical squall line were similar to those of a fast-moving tropical squall line (Figs. 1 and 2). A LLJ associated with the frontal system provided the necessary strong shear at low levels. On the front side of the squall line, front-to-rear flow prevailed at all levels with maxima at lower and upper levels and a minimum at middle levels (Fig. 2). There were many cells embedded within the squall line. Relatively weak convective downdrafts occurred between the cells and behind the main cells (Fig.1). The retrieved fields of pressure and temperature perturbations agreed well with the updraft-downdraft structure. In general, high pressure formed below the saturated, cool convective downdrafts behind the gust front, and low pressure developed underneath the convective updrafts near and above

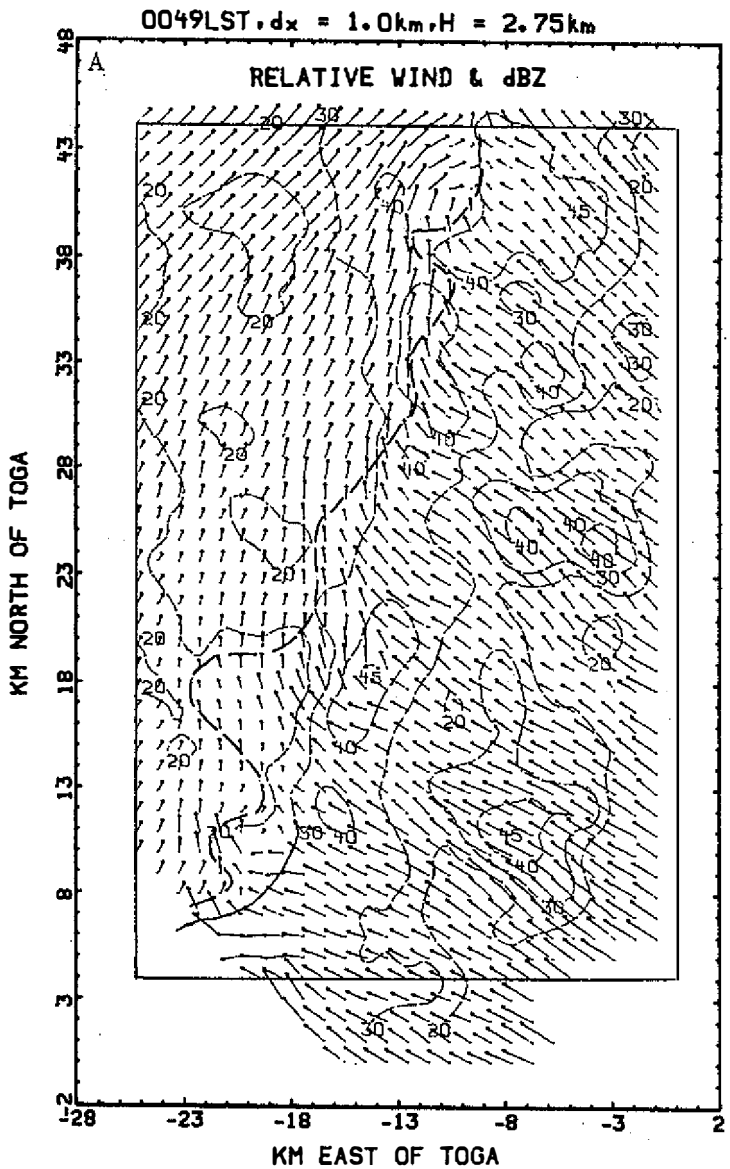

Fig. 1. Horizontal distributions of (a) storm-relative wind with reflectivity (Z) contours superimposed and (b) vertical velocity (w) at 2.75 km for 0049 LST 17 May. Contour intervals for Z and w are 10 dBZ and 2 $m\ s^{-1}$, respectively. Positive values of w are hatched. Distances are in kilometers from the TOGA radar ($\otimes$).

the gust front. Relative warming occurred in updrafts due to the latent heat release by condensation, while relative cooling prevailed in downdrafts due to the effect of evaporative cooling. A shallow layer (1-3 km) of the rear-to-front

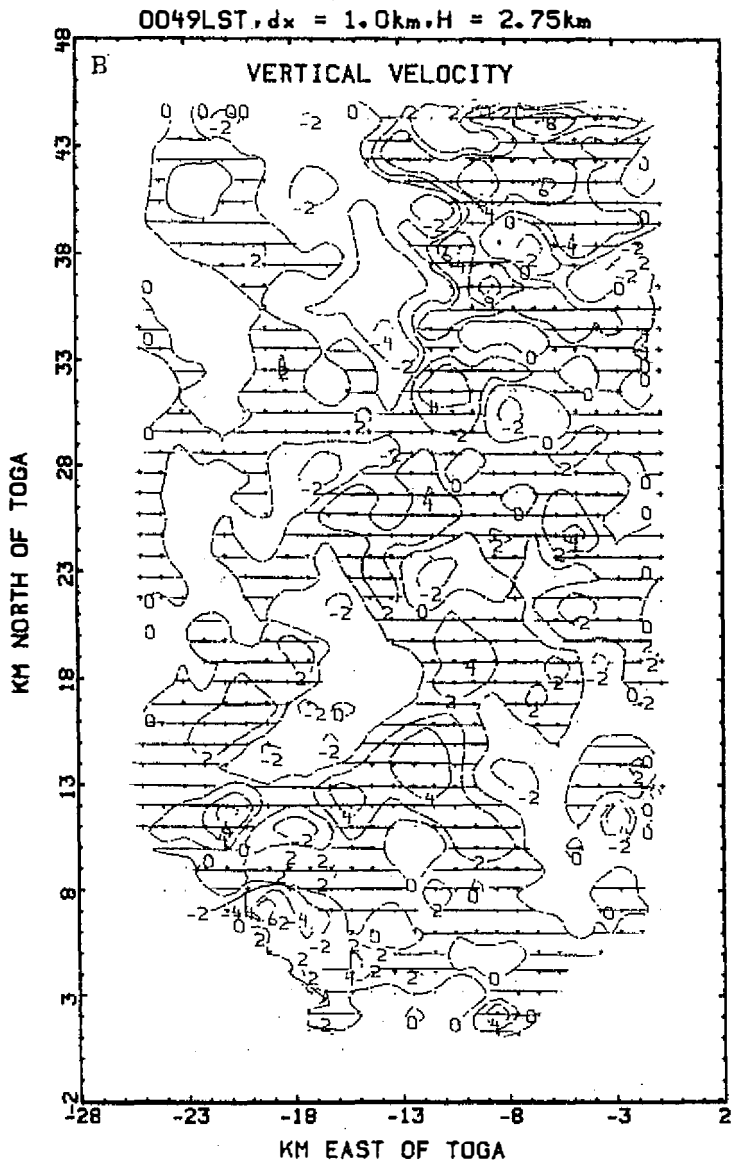

Fig. 1. (Continued)

flow, entering from the back side of the convective region, transported cooler midtropospheric air into the lower layer (Fig. 2). Part of the negatively buoyant air from the rear continued to move forward, colliding with the advancing high θ_e air in the boundary layer. As a result, new convective cells formed ahead of the old cells, thereby prolonging the life time of the squall line. The horizontal and vertical flux convergences/divergeces of horizontal momentum by the mean

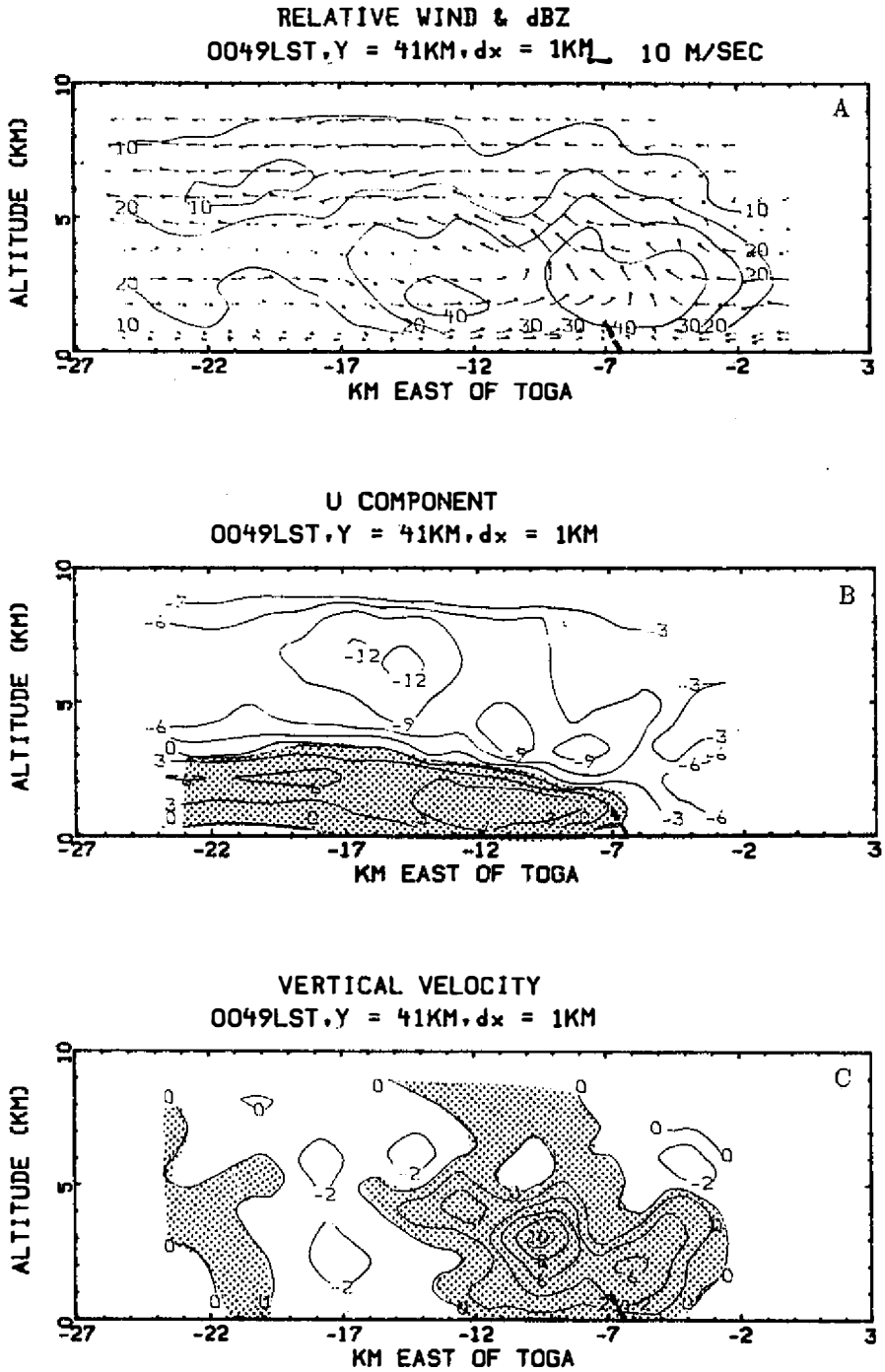

Fig. 2. The east-west cross section 41 km north of TOGA at 0049 LST 17 May, showing (a) storm-relative wind with reflectivity (Z) contours superimposed, (b) the cross-line component (u) and (c) vertical velocity (w). Contour intervals for Z, u and w are 10 dBZ, 3 $m\ s^{-1}$ and 2 $m\ s^{-1}$, respectively. Positive values for u and w are shaded. The heavy dashed line signifies the gust front.

and eddy motions are the major contributor to maintain the mean momentum.

3. METHODOLOGY

The budget equation for horizontal momentum can be derived from the following momentum equation in tensor form:

$$\frac{\partial(\rho_o u_i)}{\partial t} = -\frac{\partial(\rho_o u_i u_j)}{\partial x_j} - \frac{\partial P'}{\partial x_i} - \delta_{i3}\rho' g + f_i \tag{1}$$

where f_i are forces other than the pressure gradient force, per unit volume, $i = 1$, 2 or 3, δ_{i3} is the Kronecker constant, the subscript o denotes the (environmental) mean, the prime represents the deviation from the mean, and other symbols have their usual meanings. Decomposing the dependent variable into the (areal) mean and perturbation parts, we obtain

$$u = \overline{U} + u'; \quad v = \overline{V} + v'; \quad f_i = \overline{f}_i + f_i' \tag{2}$$

where the overbar represents the horizontal area mean. Substituting (2) into (1) and performing the bar operation, we arrived at

$$\frac{\partial \rho_o \overline{U}}{\partial t} = -\underset{A}{\frac{\overline{\partial(\rho_o uu)}}{\partial x}} - \underset{B}{\frac{\overline{\partial(\rho_o uv)}}{\partial y}} - \underset{C}{\frac{\partial(\overline{\rho_o uw})}{\partial z}} - \underset{D}{\frac{\overline{\partial P'}}{\partial x}} + \underset{E}{\overline{f}_1} \tag{3}$$

where terms A through E represent the x-component momentum flux divergence; the y-component momentum flux divergence; the vertical momentum flux divergence; the perturbation pressure gradient force; and the forces other than pressure gradients, respectively.

Equation (3) is the momentum budget equation for the u-component normal to the squall line. Each term can be assessed from the derived three-dimensional wind and retrieved pressure fields.

In a similar manner, the $\overline{V}$-momentum budget equation, parallel to the line, has the form of

$$\frac{\partial \rho_o \overline{V}}{\partial t} = -\frac{\overline{\partial(\rho_o uv)}}{\partial x} - \frac{\overline{\partial(\rho_o vv)}}{\partial y} - \frac{\partial(\overline{\rho_o vw})}{\partial z} - \frac{\overline{\partial P'}}{\partial y} + \overline{f}_2 \tag{4}$$

Note that the P' in Eq. (3) and Eq. (4) can be replaced by P_d', the deviation perturebation pressure, whenever it appears in horizontally differentiated form.

4. DISCUSSION OF RESULTS

Budgets of the horizontal momentum for both u- and v-components were computed form Eq. (3) and Eq. (4), respectively, at each analysis time for every level. The horizontal domain had dimensions of 25 km by 41 km. We employed the grid spacing of 1 km to calculate each of the terms in the budget equation. Subsequently, the time average of each term was obtained using all five analysis times of data considered.

a. Kinematic structure

At the times of analysis from 0040 to 0055 LST 17 May, the leading edge of the squall line was located approximately 10-20 km west of the west coast of Taiwan. For illustration, the field of storm-relative wind with reflectivity contours superimposed for 2.75 km at 0049 LST is shown in Fig. la. The box in the figure signifies the horizontal domain used for budget calculation. The 2.75 km level is slightly below the LLJ (3-4 km). A pronounced line of horizontal convergence is evident especially in the northern portion of the leading edge (see the heavy dashed line in Fig. la). Its position is in the high reflectivity regions. On the east side of the convergence line, storm-relative winds are predominantly from the southeast resulting in a front-to-rear (east to west) flow in the direction normal to the leading edge. On the other hand, the southwest winds prevail in the areas west of the convergence line. These winds produce a flow component from the back toward the leading edge. This rear-to-front (west to east) flow from the midtroposphere plays an important role in intiation and maintenance of the convective downdrafts (Lin *et al.*, 1990).

Fig. 1b shows the horizontal distribution of vertical velocity at 2.73 km. Inspection of Fig. 1 reveals that the convective region has many cells of updrafts and downdrafts and high reflectivities with relatively weak downdrafts between and behind. The maximum reflectivity at the leading edge is about 45 dBZ. Several new cells are seen to the east side of the main cells with reflectivities ranging from 30 to 45 dBZ. The maximum speed of updrafts is approximately 6-8 $m\ s^{-1}$ at this level. These convective updrafts are accompanied by convective downdrafts with a maximum of about $-4\ m\ s^{-1}$. A comparison of the w field at this time and that at 0043 LST (Lin *et al.*, 1990) reveals that the intensity of updrafts and downdrafts had weakened considerably as the system approached the west coast of Taiwan. The presence of topography may have played an important role in affecting the convection. This problem will be examined in our future paper.

b. Vertical cross section

The vertical cross section 41 km north of TOGA, showing the storm-relative

wind (with reflectivity contours superimposed), the cross-line (east-west) component and vertical velocity, is presented in Fig. 2. The cross section passes through the main cell and the new cell located in the northern portion of the domain. On the east side of the updrafts (right side of Fig. 2), the front-to-rear flow dominates at all levels with maxima at lower and upper levels. As described in the study by Wang *et al.* (1990), the front-to-rear environmental high θ_e air is lifted at the convergence zone in the lower troposphere, feeding the convective updrafts at the leading edge (heavy dashed line). The main updraft, with a maximum speed of 10 $m\ s^{-1}$, is tilted toward the west in the lower layer (0-4 km) and becomes almost erect higher up. A secondary updraft (new cell) to the east of the main updraft is relatively weak with a maximum speed of 6 $m\ s^{-1}$. The updraft tilt keeps water loading and evaporative cooling in the updraft to a minimum from the falling rain. As the rain falls out the updraft, it increases density of the downdraft air below the tilted updraft. The downdraft air tends to conserve its momentum, undercutting the updraft air on the downshear side of the storm. As a result of updraft-downdraft interaction in the lowest layers, the growth of the new cell occurs ahead of the old cell with a tilt into the shear instead of with it. The lifted air within the updraft column continues to rise and move westward toward the trailing stratiform region of the squall line (outside of Fig. 2) as in the tropical squall line studied by Chong *et al.* (1987).

The rear-to-front air enters from the western edge of the convective region (left side of the figure) in the 0-3 km layer (see the shaded area in Fig. 2b). This midtropospheric air is cooler than the surroundings, similar to that of a tropical squall line. As it approaches the higher reflectivity region, buoyancy of the air is decreased due to the combined effect of evaporative cooling and precipitation loading, forming a sloping downdraft in the area behind the leading edge ($-20 < x < -12\ km$). Part of the descending air carries the midtropospheric momentum forward in the boundary layer, colliding with the advancing high θ_e environmental air at the gust front ($x = -6.5\ km$). As a result of interaction between the low-level front-to-rear inflow and the opposite flow from the rear, intense convection results with a maximum speed reaching 10 $m\ s^{-1}$. A secondary updraft in conjunction with the new cell develops about 4 km east of the main (old) cell at $x = -6\ km$. The growth of the new cell ahead of the old cell due to the aforementioned updraft-downdraft interaction can often result in the storm tilting into the shear instead of with it (Rotunno *et al.*, 1988). This may explain in part why the updraft tilts toward the west against the large-scale environmental shear in the lowest layers.

c. Momentum fluxes

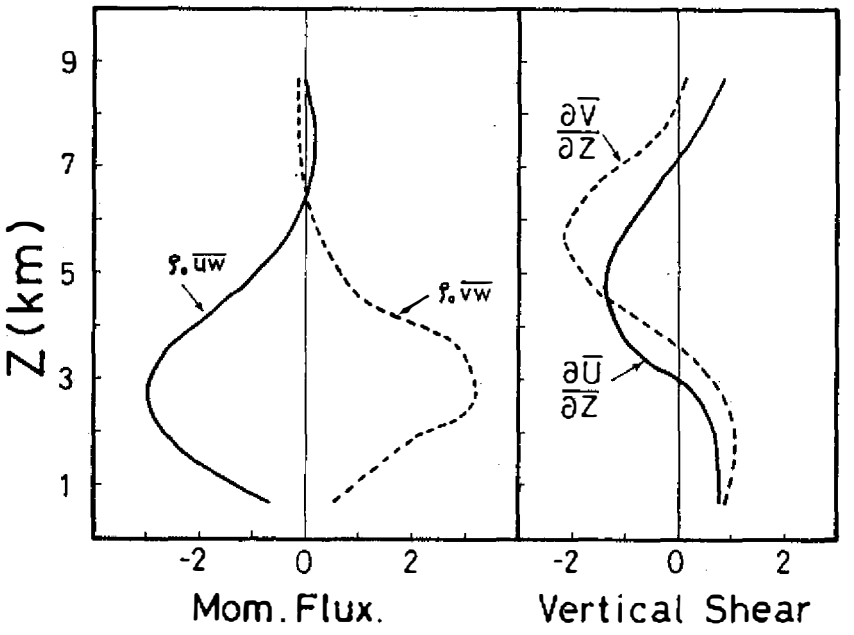

Fig. 3. Profiles of the vertical trasnport of horizontal momentum for the u-component ($\rho_o\overline{uw}$) and v-component ($\rho_o\overline{vw}$). Units are in $kg\ m^{-1}s^{-2}$ and a positive value represents an upward transport of horizontal momentum. Vertical shears of the mean horizontal momentum ($\partial\overline{U}/\partial z$ and $\partial\overline{V}/\partial z$) are also plotted with units in $10^{-3}\ s^{-1}$.

The vertical transports of horizontal momentum for both u- and v-components are presented in Fig. 3. For illustration, profiles of the mean vertical shear, $\partial\overline{U}/\partial z$ and $\partial\overline{V}/\partial z$, are also shown in Fig. 3. As noted earlier, the u-component is normal to the leading edge of the squall line and the v-component is parallel to the line. Note that profiles of $\rho_o\overline{uw}$ and $\rho_o\overline{vw}$ shown in Fig. 3 are the averages over the five analysis times considered. It is seen that a downward transport of the u-momentum dominates at heights below 6.5 km with a maximum near 3 km. This finding is in qualitative agreement with those reported in GATE and other studies. It is consistent with the westward-tilted updrafts depicted in Fig. 2. Examination of the mean vertical shear ($\partial\overline{U}/\partial z$) reveals that the vertical flux of u-momentum is countergradient in the layer between 3 and 6.5 km and is downgradient in the layer above and below. This result shows that the vertical flux of horizontal momentum normal to the line is independent of the mean vertical shear (LeMone *et al.*, 1984). Using the dual-Doppler data collected during COPT 81, Roux (1988) studied the vertical transports of horizontal momentum and thermodynamic properties in the convective region of the West Africa squall line. Results showed that

the component of momentum transverse to the line and vertical cloud potential temperature are transported against their vertical gradients, while the parallel component of momentum is transferred downgradient in agreement with those reported in the study by LeMone (1983).

Unlike the u-transport, the vertical transport of v-momentum (dashed line) is upward from the surface to 6.5 km and is downward above. The profile of $\rho_o\overline{vw}$ is countergradient in the lower layer ($z < 4$ km) and becomes downgradient in the layer between 4 and 6.5 km. The upgradient transport of v-momentum in the lower layer is different from that for tropical squall lines (LeMone, 1983; LeMone *et al.*, 1984; and Roux, 1988). We believe that the presence of the LLJ in the 3-4 km layer may have some effects on this phenomenon. This point will be further researched in the future.

From Fig. 3, we notice that the average shear in $\overline{U}$ and $\overline{V}$ through the depth of the line is negative. This means that broadly the u-momentum flux is countergradient and the v-momentum flux is downgradient. More precisely, it means that use of some sort of "cumulus friction" type of parameterization using clouds with roots in the boundary layer might be able to handle the v flux but not the u flux (LeMone, 1983).

d. Momentum budgets

As mentioned before, momentum budgets for the u-component were computed from Eq. (3) using the Doppler derived wind and retrieved pressure fields for each analysis time. The mean value for each term at a given height was subsequently obtained by taking the average over the five analysis times. Results are shown in Fig. 4 for all terms in Eq. (3) except the $\overline{f}$ term, which is shown to be much smaller than the other terms in the budget equation. Note that the x-component of horizontal momentum flux divergence (curve A) and vertical momentum flux divergence (curve C) are the most dominant terms. These two terms have the same order of magnitude but opposite sign at most levels. On the other hand, the y-component of horizontal momentum flux divergence (curve B) is relatively smaller than the x-component (curve A) at most levels. This finding is significant and is in agreement with that found in most numerical simulation studies reported in the literature. One of the major assumptions going into some of the parameterization schemes is that the $\partial/\partial y$-terms are small. Similar to curve B, the pressure gradient term (curve D) is also smaller than terms A and C, which is different from those observed during COPT 81. This result is expected since the convective system being investigated is weaker than that studied by Roux (1988), etc.

The computed tendency (COM) was obtained as a residual of the momentum equation [see Eq. (3)]. It represents the part of air acceleration that is

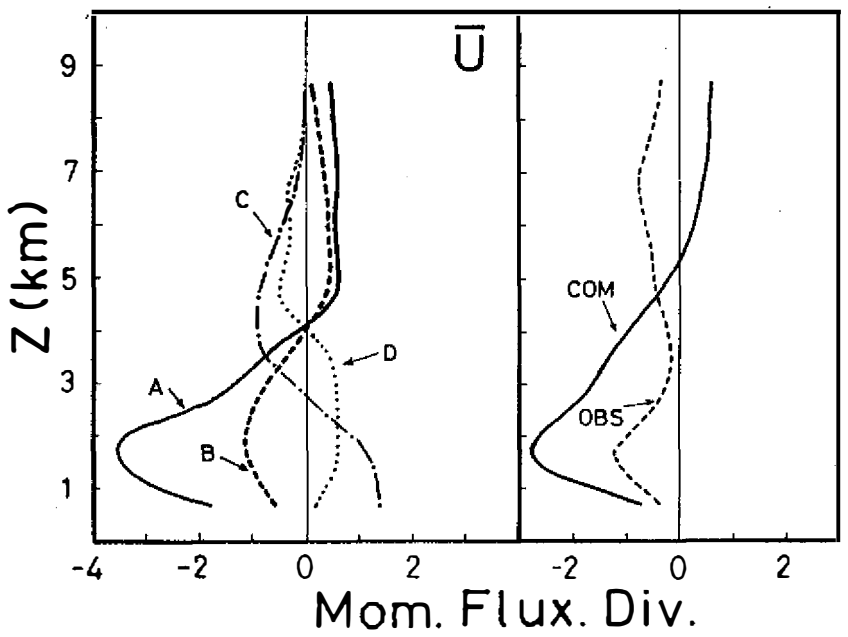

Fig. 4. Profiles of the terms in the U-momentum budget equation. Curves A-D correspond to terms A-D, respectively, in Eq. (3). The $\overline{f}_1$ term (E) is not shown since it is smaller than the other terms (A-D). The computed (COM) and observed (OBS) tendencies are also plotted. Units are in $10^{-3}\ N\ m^{-3}$.

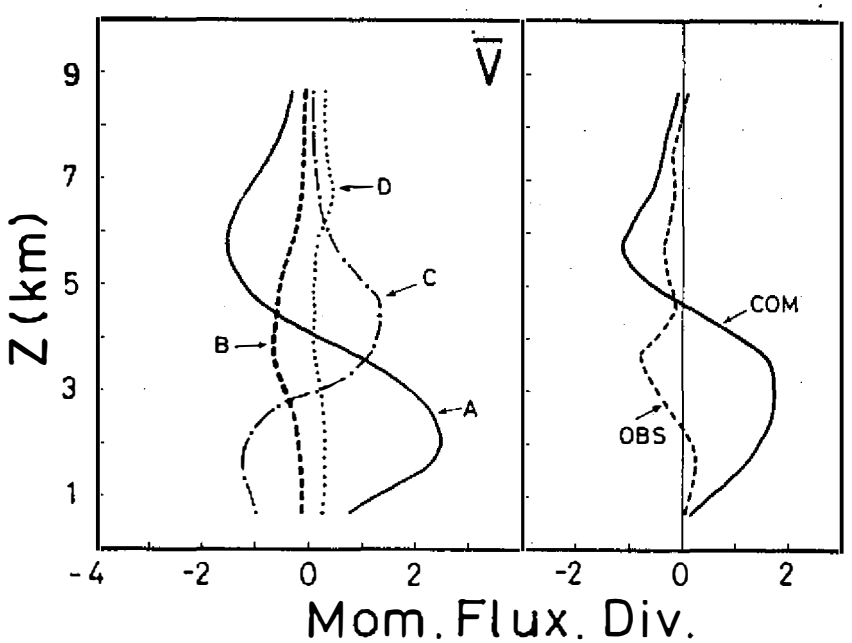

Fig. 5. As in *Fig.* 4 except for V-momentum.

not balancecd by the retrieved pressure field. It also contains indeterminate contributions of radar and numerical errors and of actual storm evolution. For comparison, the observed tendency (OBS) determined from the mean Doppler winds is also plotted in Fig. 4. Note that the observed tendencies have negative values at all levels, showing the decay of U-momentum. The computed values (COM), on the other hand, are negative at levels below 6 km and positive aloft. In the lower and middle layers, both the observed and computed tendencies are in qualitative agreement, having the same sign but different magnitude. In the upper layer, however, the computed values do not agree with the observations.

Fig. 5 shows the results for V-momentum. Like the U-component, terms A and C are the two major contributors to the local time change of V-momentum. The $\partial/\partial y$-term (curve B) is much smaller than the x-component term (curve A) at most levels. Once again, the pressure gradient term (curve D) is found to be much smaller than the other terms in (4). The computed tendencies (COM) show positive in the layers below 5 km and negative higher up. The observed tendencies (OBS) have small positive values in the lower layer ($z < 2.5$ km) and negative values higher up, indicating the weakening of the V-momentum with time in the middle and upper layers. The computed values agree with the observations only in the layers above 4.5 km and a shallow layer below 2.5 km.

As discussed in studies by Wang *et al.* (1990) and Lin *et al.* (1990), the uncertainties in the u, v, w and P'_d estimates, to some extent, will contribute to the errors in tendency calculation. In spite of these uncertainties, our study has demonstrated that some useful information in relation to the budgets and vertical transports of horizontal momentum for a subtropical squall line can still be extracted from the Doppler derived fields. Based on the findings presented in this study and our earlier TAMEX studies, we found that many structural features of an organized convection embedded within the MCS can be further undrestood using the Doppler derived winds and retrieved thermodynamic variables. Of course, the data quality and resolution must be adequate to warrant such a study. We believe that the dual-Doppler data sets considered in this study have met this requirement.

5. CONCLUSIONS

A thermodynamic retrieval method was used to study some dynamical and thermodynamical structures of a subtropical squall line on 17 May 1987. Dual-Doppler data at five consecutive analysis times in intervals of about 3 min were objectively analyzed to derive three-dimensional winds in the convective region of the squall line. Results show that the vertical transport of horizontal momentum normal to the line is downward corresponding to the west-tilted convective updrafts, while the line-parallel component results in an upward mo-

mentum transport. Budget calculations show that the horizontal and vertical flux convergences/divergences of horizontal momentum contribute largely to the growth/decay of mean horizontal momentum. The dynamical interaction between the mean flow and convective eddies in the MCS can be investigated using the momentum budget equations and vertical fluxes of horizontal momentum estimated from the Doppler derived winds.

The above conclusions are reached based solely on the case study in IOP-2. Further studies are needed to substantiate the findings presented in this study and our earlier TAMEX studies using different data sets collected during TAMEX.

Acknowledgements. The authors wish to express their appreciation to those scientists, technicians and staff members who participated in the TAMEX project. We would like to thank the National Center for Atmostancic Research (NCAR) for providing Doppler data and technical assistance. Special thanks go to the National Science Council of Republic of China and the National Science Foundation for supporting the field experiment. Discussions with M. LeMone and D. Parsons of NCAR are greatly appreciated. This work was supported in part by the Atmospheric Science Division, National Science Foundation, under NSF grant ATM-8609150. The support of Hsi Shen has come from the Defense Department, Republic of China.

REFERENCES

Chong, M., P. Amayenc, G. Scialom and J. Testud, 1987: A tropical squall line observed during the COPT 81 experiment in West Africa. Part I: Kinematic structure inferred from dual-Doppler radar data. *Mon. Wea. Rev.*, **115**, 670-694.

Lafore, J. P., J. L. Redelsperger and G. Jaubert, 1988: Comparison between a three-dimenstional simulation and Doppler radar data of a tropical squall line: Transports of mass, momentum, heat and moisture. *J. Atmos. Sci.*, **45**, 3483-3500.

LeMone, M. A., 1983: Momentum transport by a line of cumulonimbus. *J. Atmos. Sci.*, **40**, 1815-1834.

____, G. M. Barnes and E. J. Zipser, 1984: Momentum flux by lines of cumuloimbus over the tropical oceans. *J. Atmos. Sci.*, **41**, 1914-1932.

____, and D. P. Jorgensen, 1989: Precipitation and kinematic structure of the TAMEX 16 June mesoscale convective system. Part III: Analysis of in-situ data. *Preprints, TAMEX Workshop*, 110-117.

Lin, Y. J., T. C. Wang and J. H. Lin: 1986: Pressure and temperature perturbatios within a squall-line thunderstorm derived from SESAME dual-

Doppler data. *J. Atmos. Sci.*, **43**, 2302-2327.

____, ____, R. W. Pasken, H. Shen and Z. S. Deng, 1990: Characteristics of a subtropical squall line determined from TAMEX dual-Doppler data. Part II: Dynamic and thermodynamic structures and momentum budgets. *J. Atmos. Sci.*, **47**, 2382-2399.

Rotunno, R., J. B. Klemp and M. L. Weisman, 1988: A theory for strong, long-lived squall lines. *J. Atmos. Sci.*, **45**, 463-485.

Roux, F., 1988: The West Africa squall line observed on 23 June 1981 during COPT 81: Kinematics and thermodynamics of the convective region. *J. Atmos. Sci.*, **45**, 406-426.

Wang, T. C., Y. J. Lin, R. W. Pasken and H. Shen, 1990: Characteristics of a subtropical squall line determined from TAMEX dual-Doppler data. Part I: Kinematic structure. *J. Atmos. Sci.*, **47**, 2357-2381.

副熱帶颱線之動量收支：雙都普勒雷達資料分析

林永哲　沈　畦　鄭方政
美國聖路易大學地球和大氣科學系
Robert W. Pssken
美國聖路易大學數學系

摘　要

本文採用熱力反求法來了解IOP#2中一個副熱帶颱線之結構。1987年5月17日本地標準時間凌晨0040，0043，0046，0049及0052之雙都普勒雷達資料經過客觀分析後內插至45×25的水平網格上，網格間距爲1km.垂直方面自0.3至8.8公里共分不等間隔十層。垂直風速場用非彈性連續方程向下積分及變分調整的方式計算。擾動壓力場及擾動溫度場則由都普勒風場透過動量方程反求得出。這些動力場及熱力場必須經過內部檢驗後方能做進一步的詮譯。

結果顯示颱線內向西傾斜之對流上升氣流區中水平動量在垂直颱線方向之分量是向下傳送，而和颱線平行方向之分量則向上傳送。動量收支的結果可看出平均水平動量及擾動水平動量的幅合可以增强平均水平動量，而輻散則使期減弱。這些結果和copt所分析熱帶颱線很類似。本文使用都普勒風場計算之動量收支及水平動量之垂直傳輸情形有助於MCS與平均流間交互作用之了解。